Quantitative time-domain analysis of intermolecular multiple-quantum coherences (iMQC) and effects of radiation damping

S. Kirsch[1], and W. E. Hull[2]

[1]Dept. of Medical Physics in Radiology, German Cancer Research Center (DKFZ), Heidelberg, Germany, [2]Central Spectroscopy Dept., German Cancer Research Center (DKFZ), Heidelberg, Germany

Introduction

Pulse sequences of the CRAZED-type [1] generate iMQC signals of order $n > 1$, whose amplitude and time course depend on B_0 and several spin and sequence parameters [2]. In principle, iMQC signals may be used for simultaneous measurement of the diffusion constant D and relaxation times T_1 and T_2* [3]. The effects of radiation damping at high spin densities on iMQC lineshapes have been investigated for H_2O samples with long relaxation times [4]. Here we investigate quantitatively the behavior of the time-domain iMQC signals for a moderately doped water sample.

Theory

Our implementation of the CRAZED sequence was as follows: T_r - 90°$_{ph1}$ - $G(\delta)$ - Δ - $\beta°_{ph2}$ - $n\cdot G(\delta)$ - Δ - FID$_{ph3}(t')$ (1)

Following a relaxation delay (T_r), a 90° excitation with phase ph1 creates iMQC which evolves for the time $\tau = \delta + \Delta$ with spatial encoding by a gradient pulse with amplitude G and duration δ. In practise, a minimum value for the variable delay Δ will be required for the decay of eddy current effects and B_0 shifts. Following the read-out pulse β_{ph2}, the detectable SQC derived from nQ coherence is rephased by the second gradient pulse nG and evolves in the time domain $t = \delta + \Delta + t'$ under the influence of the distant dipolar field B_{DDF} and a radiation damping field B_{rd} produced by the rf current induced by the precessing M_{xy} magnetization. The combined influence of B_{DDF} and B_{rd} may result in "turbulent" spin dynamics when relaxation times are long [5]. However, for systems with short T_2*, B_{rd} should be negligible for the FID at times ($\tau + t$) >> T_2* and nonturbulent dynamics are expected. The MR signal from iMQC of order n can be written as:

$$M^+(n,\tau,t) = C_n(\tau)\cdot A_n(t); \quad \text{with } C_n = \frac{i^{n+1}}{(n-1)!2^n} M_0^n(\gamma\mu_0)^{n-1} R_{DDF}^{-(n-1)} e^{-n\tau/T_2^*}(1-\cos\beta)\sin^{n-1}(\beta) \quad \text{and } A_n(t) = e^{-t/T_2^*}\left[1-e^{-R_{DDF}t}\right]^{n-1} \qquad (2)$$

for an on-resonance singlet, where $R_{DDF} = 2k^2D + 1/T_1$, $k = \gamma G\delta$, γ= magnetogyric ratio, μ_0 = vacuum permeability, and M_0 = equil. magnetization.

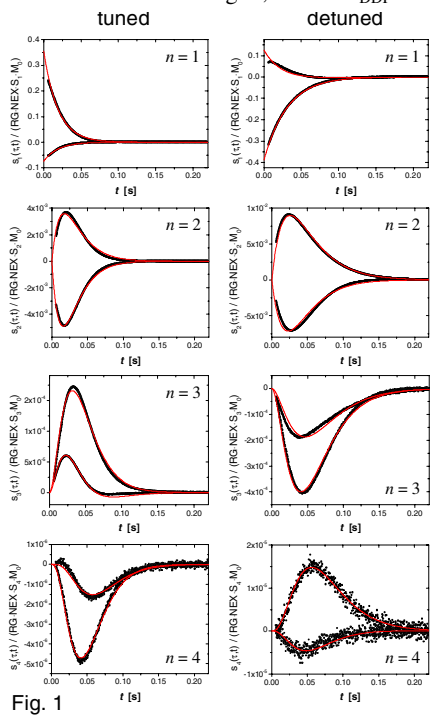

Fig. 1

Materials and Methods

All experiments were performed at ν_0(H) = 300.13 MHz (7.05 T) and 27 °C with a Bruker AM-300 spectrometer (Bruker BioSpin) equipped with imaging hardware, a microscopy probe (four-turn Helmholtz rf coil for 10-mm samples), and an actively shielded gradient system. The 10-mm sample tube contained 9.93 mM $NiSO_4$ in H_2O. Measurements were performed without deuterium lock and without B_0 compensation, with the rf coil optimally tuned (90° pulse = 8.6 µs) and detuned (90° = 82.5 µs) to minimize radiation damping. T_1 was measured by inversion-recovery (57.2 ± 0.7 ms tuned, 61.79 ± 0.04 ms detuned), T_2* by fitting a pulse-acquire FID (11.4 ± 0.01 ms tuned, 29.2 ± 0.1 ms detuned). H_2O signals derived from iMQC with n = 1 - 4 were acquired using sequence (1) on-resonance. An nQ phase cycle of $2n$ steps was employed: ph1 = (0, 1, ... $2n$–1)·(360°/$2n$); ph2 = 0°; ph3 = (add, sub)$_n$. Parameters were: spectral width 2994 Hz, 4K complex points, 16-bit ADC, filter bandwidth = 50 kHz (n = 1 - 3) or 25 kHz (n = 4); acquisition time = 684 ms; T_r = 1.0 s, β = 90°, G = 20.85 mT/m, δ = 1 ms; Δ = 5 ms (to avoid the B_0 shift transient); excitations (NEX) = 16 - 640 (depending on n). The acquired time-domain quadrature signals s_n were scaled with calibrated receiver gain factors (RG) and NEX and fitted by a Levenberg-Marquardt algorithm (ORIGIN®, OriginLab, USA) according to

$$s_n(\tau,t)/(\text{RG}\times\text{NEX}) = S_n\cdot C_n(\tau)\cdot A_n(t)\cdot\exp\left[-i(\alpha+2\pi\Delta f\, t)\right], \qquad (3)$$

using Eq. 2. Only three variables were fitted: S_n (abs. intens. scaling factor), α (an RG-dependent phase constant), and T_2*. All other defined or measured constants were fixed: M_0 = 0.02257 A/m (H_2O), D = 2.44 × 10^{-9} m^2 s^{-1} (T = 300 K), T_1, δ, G, τ, β, Δf (freq. offset from peak picking, <2 Hz).

Results & Discussion

Fig. 1 presents plots of the real (■) and imaginary (○) scaled data points of Eq. 3, normalized by division by S_nM_0. The corresponding fitted curves (—) showed good basic agreement (r^2 > 0.91 for all) with only minor systematic deviations (lineshape asymmetry). In **Table 1** the fitted parameters S_n and $\alpha-\alpha_{RG}$ (phase corrected for measured RG dependence) should ideally be constant for all n since all amplitude and phase factors depending on n are incorporated in C_n and A_n of Eq. 3. Reasonably constant S_n and phase were achieved for n = 1 - 4 in the detuned case, without radiation damping. The amplitude and phase factors were less consistent with theory in the tuned case, particularly for n = 1, suggesting incomplete nQ filtering, rf inhomogeneity, or pulse imperfections exacerbated by radiation damping. It is noteworthy that T_2* values were essentially *independent* of n and, for the detuned case, agreed well with the limiting value of 29.73 ± 0.09 ms obtained for a pulse-acquire FID with the coil completely detuned (R_2* = 33.6 s^{-1}). For the tuned case T_2* values were shortened to 19 - 20 ms, also independent of n. The contribution of radiation damping was R_{rd} = 54.1 s^{-1} for a pulse-acquire FID (R_2* = 87.7 s^{-1}) and R_{rd} = ca. 18 s^{-1} for iMQC (R_2* = 50 - 53 s^{-1}). Thus, the contribution of radiation damping to R_2* of iMQC signals was about one-third of that observed for a normal FID, and surprisingly the same for signals differing by five orders of magnitude.

Table 1	**tuned**			
n	**1**	**2**	**3**	**4**
S_n [10^4 au]	34.1 ± 0.6	66.7 ± 1.0	66.8 ± 0.7	72.7 ± 0.5
***T*$_2$* [ms]**	**18.9 ± 0.03**	**18.8 ± 0.03**	**19.6 ± 0.05**	**20.2 ± 0.05**
$\alpha-\alpha_{RG}$ [°]	253.8 ± 0.05	272.8 ± 0.70	271.8 ± 0.09	278.0 ± 0.93
	detuned			
S_n [10^4 au]	3.57 ± 0.04	3.02 ± 0.03	3.04 ± 0.02	2.99 ± 0.20
***T*$_2$* [ms]**	**29.9 ± 0.15**	**30.2 ± 0.04**	**29.7 ± 0.05**	**29.9 ± 0.34**
$\alpha-\alpha_{RG}$ [°]	79.9 ± 0.12	77.3 ± 0.44	79.1 ± 0.27	70.6 ± 8.8

References: [1] Warren WS, *et al.* Science 262 (1993) 2005-2009. [2] Ramanathan C, *et al.* J Chem Phys 114 (2001) 10854-10859. [3] Barros Jr W, *et al.* J Magn Reson 178 (2006) 166-169. [4] Zheng B, *et al.* J Chem Phys 123 (2005) 074317. [5] Huang SY, *et al.* J Chem Phys 116 (2002) 10325-10337.